Journal of Hydrology 560 (2018) 275–288

Contents lists available at ScienceDirect

Journal of Hydrology

journal homepage: www.elsevier.com/locate/jhydrol

Research papers

Recharge processes and vertical transfer investigated through long-term monitoring of dissolved gases in shallow groundwater

V. de Montety [a,*], L. Aquilina [b], T. Labasque [b], E. Chatton [b], O. Fovet [c], L. Ruiz [c], E. Fourré [d], J.R. de Dreuzy [b]

[a] HSM, Univ Montpellier, CNRS, IRD, Montpellier, France
[b] OSUR-Géosciences Rennes, Université Rennes1-CNRS, 35042 Rennes, France
[c] INRA, Agrocampus Ouest, UMR1069 Sol Agro et hydrosystème Spatialisation, 35000 Rennes, France
[d] LSCE, UMR8212, IPSL/CEA – CNRS – UVSQ, Saclay, France

ARTICLE INFO

Article history:
Received 20 July 2017
Accepted 27 February 2018
Available online 8 March 2018
This manuscript was handled by C. Corradini, Editor-in-Chief, with the assistance of Philippe Negrel, Associate Editor

Keywords:
CFCs
SF_6
Noble gases
Residence time
Groundwater recharge processes
Flow model
Agricultural catchment
Vadose zone

ABSTRACT

We investigated temporal variations and vertical evolution of dissolved gaseous tracers (CFC-11, CFC-12, SF_6, and noble gases), as well as $^3H/^3He$ ratio to determine groundwater recharge processes of a shallow unconfined, hard-rock aquifer in an agricultural catchment. We sampled dissolved gas concentration at 4 locations along the hillslope of a small experimental watershed, over 6 hydrological years, between 2 and 6 times per years, for a total of 20 field campaigns. We collected groundwater samples in the fluctuation zone and the permanently saturated zone using piezometers from 5 to 20 m deep. The purpose of this work is *i*) to assess the benefits of using gaseous tracers like CFCs and SF6 to study very young groundwater with flows suspected to be heterogeneous and variable in time, *ii*) to characterize the processes that control dissolved gas concentrations in groundwater during the recharge of the aquifer, and *iii*) to understand the evolution of recharge flow processes by repeated measurement campaigns, taking advantage of a long monitoring in a site devoted to recharge processes investigation.

Gas tracer profiles are compared at different location of the catchment and for different hydrologic conditions. In addition, we compare results from CFCs and $^3H/^3He$ analysis to define the flow model that best explains tracer concentrations. Then we discuss the influence of recharge events on tracer concentrations and residence time and propose a temporal evolution of residence times for the unsaturated zone and the permanently saturated zone. These results are used to gain a better understanding of the conceptual model of the catchment and flow processes especially during recharge events.

1. Introduction

As nitrates have become a major environmental threat in agricultural areas, numerous works evaluate mechanisms controlling NO_3^- exportation from catchment and emphasize the key role of the shallow groundwater (Böhlke and Denver, 1995; Creed and Band, 1998; Martin et al., 2006; Molenat et al., 2002). In particular, these studies show that catchment can present an important time lag in response to variation of the NO_3^- input signal. Although physical characteristics of shallow groundwater are pointed out to explain this delay, mechanisms involved are still debated. A better knowledge of this time lag, through the evaluation of the residence time of groundwater is thus crucial for managing groundwater in small agricultural catchments.

Recent results obtained using natural solutes and/or their isotopic composition as tracers, pointed out that small catchments show variable residence times that can surprisingly exceed several years (Hrachowitz et al., 2013; Kendall and McDonnell, 1998; Kirchner et al., 2001; Ruiz et al., 2002a). These methods were based on opposite trends observed between the nitrate concentrations in drainage water and in stream water (Ruiz et al., 2002a) or on spectral analysis of the input–output signal of chemical compound (Kirchner et al., 2001; Molénat et al., 2000; Neal and Kirchner, 2000) that require a high frequency monitoring of rain inputs for a long period which is rarely available.

Another approach to estimate response time to changes in agricultural practices consists in numerical modelling. Again, transit times greater than one year and up to 14 years in headwater catchments have been derived from mechanistic groundwater modelling (Basu et al., 2012; Martin et al., 2006; Molénat and Gascuel-Odoux, 2002) or lumped and parsimonious model and time series of nitrate concentration in streams (Fovet et al., 2015; Ruiz et al., 2002b). All these approaches use the approximation of Dupuit-Forsheimer which reproduces the water dynamic of the catchment, but assume a perfect and instantaneous vertical mixing

* Corresponding author.
E-mail address: veronique.de-montety@univ-montp2.fr (V. de Montety).

https://doi.org/10.1016/j.jhydrol.2018.02.077
0022-1694/

of groundwater neglecting vertical flows. In addition, in numerous models, individual storm events are neglected and only base flow is considered (Fovet et al., 2015; Ruiz et al., 2002b). Although these models reproduce seasonal and inter-annual nitrate variations, processes inducing temporal concentration variations at shallow depth are still poorly understood, especially after storm events.

An interesting alternative to obtain additional information on water dynamics is to analyze anthropogenic atmospheric gases. Industrial production of CFCs and SF_6 started in the 1940s and 1960s respectively which makes these dating tracers suitable for the study of post-war diffuse pollution in agricultural catchments (IAEA, 2006). However, following Montreal protocol in 1987, stagnation and then decrease of atmospheric CFCs concentrations over the past two decades have induced higher uncertainties in dating of young shallow groundwater since two different recharge dates can be derived from a single gas concentration (rising or falling part of the atmospheric curve (CMDL/NOAA)). Therefore, the combined use of other dating tracers like SF_6 (whose input atmospheric function is always rising) and $^3H/^3He$ (a radioactive parent/daughter clock method which does not require the knowledge of the ^3H input function) allows reducing uncertainties (Darling et al., 2012; Newman et al., 2010; Suckow, 2014). Another advantage of the anthropogenic gas tracers is to help conceptualizing flow and mixing processes of the studied groundwater system (Darling et al., 2012; Suckow, 2014). It is common to use lumped parameter models which fit the data to a conceptual model of defined flow, among which the most commonly used are piston (PFM), binary mixing (BMM) or exponential mixing (EM) (Maloszewski and Zuber, 1982). While each different tracer will give an apparent tracer age, stating the model used to interpret tracers concentrations will allow defining a Mean Residence Time (MRT) corresponding to the weighted average of the age distribution (Suckow, 2014).

Numerous authors used CFCs and SF_6 to obtain a better understanding of pollutant-transfer processes and to predict the most likely evolution of groundwater quality with respect to diffuse agricultural pollution (Böhlke, 2002; Gooddy et al., 2006; Katz et al., 2001; Koh et al., 2006). Gooddy et al. (2006) used the comparison of the spatial distribution of different tracers and lumped parameter models to discriminate groundwater flow regimes in different parts of the aquifer and thus improved their conceptual model. Kolbe et al. (2016) coupled groundwater modelling with CFC age dating to classify local groundwater circulation in an unconfined aquifer. Recent studies in hard-rock aquifers in Brittany provided a potential regional distribution of residence times as well as a reconstruction of NO_3^- concentration in recharge water (Aquilina et al., 2012; Ayraud et al., 2008).

Temporal variability of residence time in the first meters of the aquifer usually receives less attention though being essential to further assess recharge processes in the critical zone. For instance, few studies focus on vertical variation of CFCs in shallow groundwater although it is a key parameter to constraint solute transfer from soil to the water table and within the aquifer (Cook et al., 1996, 1995; Le Gal La Salle et al., 2012). Moreover, no study to date investigates the temporal variability of dissolved CFCs and SF_6 concentrations at a single location over several hydrologic cycles nor how robust is the conceptual model over time. Such information can be used to evaluate how residence time changes with varying recharge conditions.

In this context, the scope of this paper is *i*) to assess the benefits of using gaseous tracers like CFCs and SF6 to study very young groundwater with flows suspected to be heterogeneous and variable in time, *ii*) to characterize the processes that control dissolved gas concentrations in groundwater during the recharge of the aquifer, and *iii*) to understand the evolution of recharge flow processes by repeated measurement campaigns, taking advantage of a long monitoring in a site devoted to recharge processes investigation (Legout et al., 2005; Rouxel et al., 2011).

To address these issues, we focus on a shallow unconfined aquifer in a small experimental catchment in Brittany (West of France) where flow processes and nitrate dynamic have been extensively studied giving a strong knowledge on water quality (Martin et al., 2006, 2004; Rouxel et al., 2011; Ruiz et al., 2002b). We investigate dissolved CFCs and SF_6 gases concentrations during 6 hydrological cycles at different depths ranging from 4 to 20 m below ground level. Gas tracer profiles are compared at different locations of the catchment and for different hydrologic conditions. We compare CFCs and $^3H/^3He$ apparent ages and discuss flow model that best explains tracer concentrations and origin of apparent age discrepancies between age dating tracers. Then we discuss the influence of recharge events on tracer concentrations and residence time and propose a temporal evolution of residence times for the unsaturated zone and the permanent groundwater of the catchment. These results are used to gain a better understanding of the conceptual model of the catchment and flow processes especially during recharge events.

The originality of this work is thus *i*) to use a detailed analysis of long-term time-series of dissolved gas tracers (CFC-11, CFC-12, SF_6 as well as recharge temperature and excess air deduced from noble gases concentrations); *ii*) to investigate their temporal evolution in vertical profiles ranging from 0 to 20 m below ground level.

2. Methods

2.1. Site description

Kerrien site is a small experimental catchment (0.095 km^2) located closed to the sea in an intensive agricultural area southwest of Brittany, France (Fig. 1). This site is part of the French observatory network RBV (http://rnbv.ipgp.fr/) and belongs to the Environmental Research Observatory AgrHys (http://www6.inra.fr/ore_agrhys_eng/) devoted to studies of response times of hydro-chemical fluxes under changing agriculture.

The study site is representative of hard rock catchments. It has been previously described by Martin et al. (2004). The fissured and fractured granitic bedrock is overlain by a regolith of an estimated average thickness of 20 m (Martin et al., 2004). The regolith constitutes the main unconfined, shallow aquifer, with a hydraulic conductivity ranging from 9.10^{-6} to $5.10^{-4} m{\cdot}s^{-1}$ and a total porosity of 0.4% (Rouxel et al., 2012). The hillslope of the catchment shows a topographic gradient varying from 14% upslope to 5% downslope. Groundwater table roughly follows the topographic slope. It comes up to the ground level downslope while upslope, a zone of about 2 m thickness remains permanently unsaturated. The surface runoff is negligible on the hillslopes and the shallow groundwater provides most of the stream flow with a base flow index about 90% (Ruiz et al., 2002b). Groundwater table level displays large seasonal fluctuations ranging from less than one meter downslope to 4 to 6 m upslope.

The climate is oceanic. Mean annual rainfall for the period 2003–2010 was 1033 ± 186 mm, slightly lower than the mean annual rainfall of 1185 mm over the decade 1992–2002 (Molenat et al., 2008). The interannual variability is large with rainfall in 2005 (616 mm) being half of rainfall in 2010 (1220 mm). Mean annual PET is less variable with a mean annual value of 704 ± 19 mm. The average maximum and minimum monthly rainfall occurs in November and September (143 mm and 47 mm respectively). Recharge period extends from November to March but it can vary slightly depending on the yearly rainfall pattern.

Groundwater chemical composition has been extensively studied since the early 1990s in this site (Martin et al., 2004;

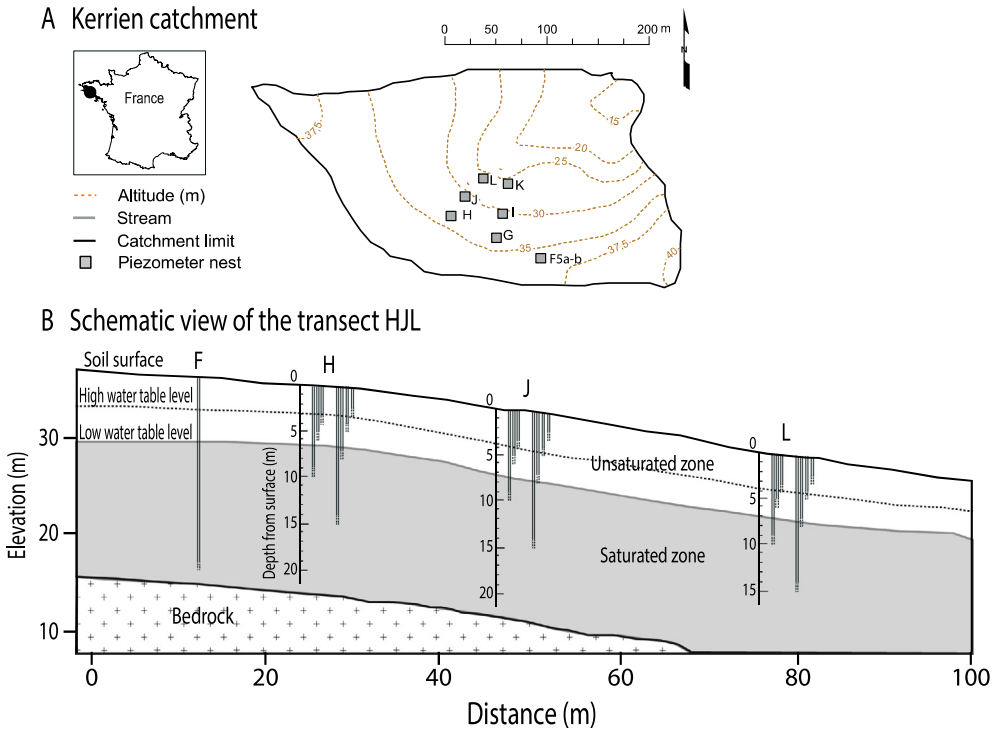

Fig. 1. (A) Topography of the Kerrien catchment with (B) a schematic view of the transect F, H, J, L and the piezometer nests.

Martin et al., 2006; Molenat et al., 2008; Rouxel et al., 2011, and references therein). Groundwater has been affected by diffuse pollution due to intensive agriculture and breeding over the last 40 years (Ruiz et al., 2002b). The groundwater display high nitrate concentrations upslope and below 2 m downslope (Molenat et al., 2008). Nitrate fluxes and seasonal variability have been analyzed in previous works (Martin et al., 2004, 2006; Rouxel et al., 2011; Ruiz et al., 2002b).

The site was instrumented since the early 1990s. In December 2004, 42 nested piezometers from 3 to 15 m depth were drilled at three different positions along the slope. They were organized in two transects along the hillslope, each containing 3 nests of 7 piezometers (Fig. 1). The shallow wells (3 and 4 m) were screened on the last 50 cm only and the other ones (5, 6, 8, 10 and 15 m) were screened on the last meter, allowing precise sampling at the different depths (Rouxel et al., 2011). This study focuses on the first transect H, J, L. After the installation of the piezometers, the catchment received low input of mineral fertilizer or manure (Rouxel et al., 2011). In addition, we sampled a 20 m deep piezometer (F), screened between 19 m and 20 m, and drilled in 2001 upslope near the catchment divide (Martin et al., 2004).

2.2. Sampling and chemical analyses

2.2.1. Field sampling

Groundwater samples were collected from the piezometers at the 3 nests H, J, L at depth ranging from 5 to 15 m and from the piezometer F at 20 m depth (Table 1). Twenty sampling surveys have been realized during the monitoring period covering 6 hydrological cycles. More than 170 samples were collected for CFCs analyses (2005–2010) and 110 samples for SF_6 (2006–2010). Noble gases have been sampled since 2007. The number of samples per piezometer varied from 3 to 5 samples for shallow piezometers (5 m) to up to 16 samples in the permanent groundwater (10–15 m).

Groundwater samples were collected with a submersible MP1 Grundfos pump connected to a nylon tubing after stabilization of their physico-chemical parameters (temperature, specific conductivity, pH and ORP). CFCs and SF_6 samples were collected without atmospheric contact in glass ampoules of 20 ml (CFCs) and 500 ml (SF_6) closed with two PTFE three-way valves for samples before March 2007 and in stainless-steel ampoules of 40 ml (CFCs) and 300 ml (SF_6) closed with two stainless-steel three-way valves since then. Noble gases were sampled in 500 ml glass bottles after purging three times the bottle volume under water in a bucket. Bottles were closed with rubber caps and sealed with metal ring. All sampling ampoules were rinsed 3 times before collecting water. Physico-chemical parameters were simultaneously measured and major elements collected for each sampling period. Samples were filtered in the field (0.45 μm) and kept refrigerated prior to analyses. In addition, for four sampling campaigns (June07, Dec08, Apr and Oct09) specific sampling was dedicated to $^3H/^3He$ analyses, representing 39 samples. Samples for ^3H analyses were collected in 500 ml Pyrex bottles, baked at 75 °C and pre-filled with argon. Samples for He analyses were collected using standard refrigeration grade 3/8″ copper tubes sealed by metal clamps at both ends.

Water table levels were recorded at 15 min intervals in the deepest piezometers (H15, J15, and L15). Precipitation, and the parameters required to calculate potential evapotranspiration by the Penman formula (mean temperatures, mean relative humidity, global radiation, wind velocity) were recorded at hourly frequency 700 m away from the study site.

2.2.2. Lab analyses

Anthropogenic and noble gases analyses were realized in Geosciences Rennes laboratory as detailed in Labasque et al. (2008). CFCs and SF_6 were extracted following the purge and trap method and quantified by gas chromatography with electron capture detection. The analyses are within a precision of 3% for CFC-11 and CFC-12 and 5% for SF_6. Noble gases (Ne, Ar) and N_2 were extracted by head-space and measured by gaz chromatography with a catharometer detector (μGC 3000 – SRA) with a precision of 5%. Major anions (Cl^-, SO_4^-, NO_3^-) were analyzed with an

Table 1
Number of sample (No), mean values and standard deviation (STDV) obtained for CFC-11, CFC-12, SF_6 and $^3H/^3He$, per nest and per depth. For CFCs and SF6, both mixing ratio and apparent tracer ages are given. The relative standard deviation (RSD) is also given for CFCs and SF_6.

		CFC-11						CFC-12						SF_6				$^3H/^3He$		
Atmospheric maximum		272,8						546,32						6,99						
		Mixing ratio (pptv)				App. Age (Years)		Mixing ratio (pptv)				App. Age (Years)		Mixing ratio (pptv)				App. Age (Years)		
Depth	Name	**No**	Mean	STDV	RSD	Mean	STDV	**No**	Mean	STDV	RSD	Mean	STDV	**No**	Mean	STDV	RSD	**No**	Mean	STDV
	F	**19**	247,1	10,1		19,3	2,1	**16**	491,7	33,2		17,6	3,6	**11**	6,4	1,5		**4**		
15	F5a	**8**	252,6	7,9	3%	18,4	2,4	**6**	483,7	42,7	9%	16,8	5,4	**4**	5,1	0,9	18%			
20	F5b	**11**	243,1	9,9	4%	20,0	1,6	**10**	496,5	27,5	6%	18,2	1,8	**7**	7,1	1,2	17%	**4**	8,3	0,8
	H	**63**	253,3	22,5		6,8	7,5	**51**	498,9	47,3		9,4	8,6	**38**	7,4	1,9		**14**		
5	H5	**5**	246,5	17,1	7%	2,8	4,6	**3**	518,6	22,4	4%	−1,3	2,5	**2**	7,6	0,4	5%			
6	H6	**12**	230,8	23,9	10%	0,4	2,5	**7**	492,1	43,2	9%	3,5		**5**	6,2	2,1	34%	**2**	1,3	1,3
8	H8	**15**	251,9	15,2	6%	3,2	4,2	**13**	475,3	72,8	15%	−3,8	0,4	**9**	6,7	1,2	17%	**4**	5,3	2,9
10	H10	**16**	260,5	19,5	8%	4,6	4,9	**13**	508,0	37,0	7%	2,6	3,8	**9**	8,2	1,9	23%	**4**	4,8	1,3
15	H15	**14**	267,3	19,7	7%	18,0	3,2	**13**	510,9	25,4		16,0	3,1	**11**	7,6	2,3		**4**	12,3	2,4
	J	**51**	255,1	19,8		9,3	7,8	**46**	493,3	39,4		14,6	7,6	**39**	7,4	1,7		**10**		
5	J5	**4**	251,9	24,9	10%	7,0	6,6	**3**	514,7	67,6	13%	−2,5		**3**	7,9	0,9	12%			
6	J6	**7**	248,0	21,9	9%	4,3	4,8	**6**	499,8	40,2	8%	−3,0		**5**	7,0	0,7	11%	**1**	5,3	
8	J8	**10**	249,1	28,5	11%	5,4	7,0	**8**	502,8	39,5	8%	4,5		**7**	7,4	1,9	26%	**2**	6,2	1,6
10	J10	**15**	259,3	14,7	6%	5,3	4,8	**13**	493,5	22,9	5%			**11**	7,6	2,4	32%	**3**	6,0	2,1
15	J15	**15**	258,9	15,3	6%	19,1	2,0	**16**	481,9	45,3	9%	17,4	3,7	**13**	7,4	1,4	18%	**4**	6,2	2,0
	L	**41**	249,9	21,4		9,1	8,1	**35**	485,7	49,0		14,5	7,9	**24**	7,7	2,2		**11**		
5	J5	**3**	246,5	10,5	4%	3,3	0,4	**3**	500,4	35,8	7%	−0,5		**1**	8,2					
6	J6	**5**	237,3	20,1	8%	1,1	2,0	**5**	494,6	41,5	8%	−1,0		**3**	5,8	1,7	30%	**1**	2,2	
8	J8	**9**	242,4	20,6	8%	4,9	2,5	**8**	466,3	86,7	19%			**4**	7,7	3,5	46%	**3**	4,4	1,5
10	J10	**12**	251,0	21,5	9%	5,1	5,2	**9**	490,2	33,0	7%			**8**	7,4	2,4	33%	**3**	7,3	1,4
15	J15	**12**	260,6	21,8	8%	19,3	2,1	**10**	488,3	27,4	6%	17,6	3,7	**8**	8,7	1,3	15%	**4**	10,3	0,8
	Total	**174**	252	20,5		9,9	8,2	**148**	493	43,9		13,5	7,8	**112**	7,4	1,9		**39**	6,8	3,2

automated Dionex DX-100 Ion Chromatograph with a precision better than 5%. Tritium and noble gas isotopes (^3He, ^4He and ^{20}Ne) were analyzed at LSCE (Saclay, France) with a MAP-215-50 mass spectrometer using routine procedures (Jean-Baptiste et al., 2010, 1992). ^4He and ^{20}Ne isotopes were measured to assess excess air and radiogenic contribution and derive the tritiogenic ^3He component. Dissolved He and Ne were first extracted under vacuum into sealed glass tubes. The measurements were calibrated with an air standard. The water for ^3H determination was degassed and stored to allow for ^3He ingrowth before mass spectrometry measurement. Mean uncertainty is about 5% for ^3H, and between 1% and 1.5% for He and Ne isotopes.

2.3. Data analyses

Uncertainty of apparent CFCs and SF6 age determination relies first on the calculation of atmospheric mixing ratio (pptv) in recharge water. This calculation requires the groundwater recharge elevation and the recharge temperature. The studied catchment can be assumed as a simple homogeneous system with an average elevation of 30 m above sea level and low topographic variation within the catchment area (<10 m). Influence of recharge elevation is reported to be small for elevation variation below 1000 m (IAEA, 2006), the recharge elevation has thus a minor impact in CFCs determination in this study. The recharge temperature can be assumed to be close to the mean annual air temperature ±1 °C (Cook et al., 2006; Herzberg and Mazor, 1979). During the monitoring period, the mean annual air temperature is 11.9 ± 0.4 °C, in good accordance with previous work (11.4 °C; Ruiz et al., 2002b), with mean monthly temperature ranging from 6.4 °C in February to 16.7 °C in July.

Ne and Ar concentrations were also used to estimate Noble Gaz recharge Temperature (NGT) as well as excess air. Two methods were used: (i) Ar/Ne chart (Heaton and Vogel, 1981) (ii) an inversion model (Aeschbach-Hertig et al., 2000; Stute et al., 1995) using, Ne, Ar and N2 to compute the recharge parameters including recharge temperature, excess air and fractionation using either a closed equilibrium or a partial re-equilibration model (Chatton et al., 2016). A comparison of the three computations showed only a slight difference of recharge temperature (0.6 °C). Therefore, the closed equilibrium model has then been used.

At the water table (6m), water temperature varies between 11 ± 1 °C in March to 13 ± 1 °C in the period October-December. Mean NGT is about 10 °C with variations between 7.5 °C and 17 °C with most of the data comprise between 7 °C and 12.5 °C. There is a strong variation of NGT (±3 °C) compared to water temperature in wells with numerous data below the lower measured water temperature. When considering impact of recharge temperature on calculated CFCs ratios, it appears that the use of low temperature value (7 °C) increases solubility and then decreases CFCs ratios for the same concentration in water. As a consequence, permanent groundwater shows older apparent tracer ages, (162pptv -26yrs at 7 °C compare to 214pptv -20yrs at 11.9 °C for CFC-11) and ratios in shallow water become too low for estimating age on the recent part of the atmospheric curve. Finally, we do not have NGT for all the dataset since noble gas measurement started only in 2007. For all these reasons and to not introduce a bias in the CFCs ratios calculation at the different sampling date, mean annual air temperature has been used for CFCs and SF6 ratios calculation. NGT temperature estimated with only two noble gases (Ne and Ar) gives too large uncertainties. Kr and Xe determination should be developed. N2 utilization in this agricultural watershed should also introduce uncertainties on NGT. The sensitivity of apparent age determination to a variation of 1 °C of recharge temperature is small. The sensitivity for CFC-11 is <2 years. $°C^{-1}$ for recharge before 1994 and 5 years. $°C^{-1}$ in average for recharge after 1994. For CFC-12, only recharge prior to 2002 were determined with apparent ages precisions about 2 years $°C^{-1}$.

SF_6 data were corrected for the influence of excess air using Ne concentrations according to the methodology proposed by Aeschbach-Hertig (2004). For sample collected before the first noble gases sampling, a mean value of excess air was calculated

for each piezometer using samplings from 2007 to 2010. The influence of excess air was found to be negligible for CFCs and has thus been neglected.

The calculated mixing ratios were then compared to atmospheric mixing curves to estimate the apparent age of water. Considering the rural location of the study site, no local contaminations were expected (Ayraud et al., 2008). The CMDL/NOAA values were thus used as input function for CFCs and SF_6. CFC-11 concentrations and to a lesser extent CFC-12 concentrations fall close to the maximum atmospheric air concentration due to the relatively short residence time of water in this shallow aquifer. Consequently, for samples with concentration ranging from 240pptv to 272pptv for CFC-11 and from 530pptv to 546pptv for CFC-12, 2 apparent recharge dates could be attributed (before or after the atmospheric maximum value). If all samples had been attributed to the same portion of the atmospheric curve, the same range of apparent age would have been attributed to shallow (4–6 m) and deep samples. Moreover, when considering apparent recharge date before the maximum atmospheric concentration for samples from 6–10 m, a general decrease of apparent age with depth was observed. These two results were found unrealistic and were in strong disagreement with observed Cl^- evolution and prior knowledge on the hydrogeological context. To decide which portion of the atmospheric curve should be used, we used the vertical evolution of $^3H/^3He$ age. $^3H/^3He$ analysis show low age for samples at 6 m (<2 yrs) and a general increase of age with depth (~0.75 yrs/m). Consequently, recharge dates were determined using the portion of the atmospheric curve before the maximum for deep groundwater (15–20 m) and the portion of the atmospheric curve after the maximum for the other depth (10, 8, 6, 5 m).

The $^3H/^3He$ age was computed using usual methodology (Schlosser et al., 1989). The $^3H/^3He$ age τ is defined as $\tau = \lambda^{-1}\mathrm{Ln}(1 + {}^3He_{tri}/{}^3H)$, where λ is the decay constant for tritium; ^3H is the measured tritium concentration expressed in Tritium Units (TU) and $^3He_{tri}$ is the fraction of the total ^3He produced by ^3H decay. $^3He_{tri}$ is the difference between the measured ^3He concentration and the sum of ^3H concentrations from atmospheric ($^3He_{atm}$) and terrigenic ($^3He_{ter}$) origins. The atmospheric component reflects both the gas dissolved at the solubility equilibrium and an excess air component as ubiquitously observed in groundwater (Kipfer et al., 2002 and references therein). $^3He_{atm}$ and $^3He_{ter}$ can be deduced from the measured concentrations of He and Ne, $^4He_{meas}$ and $^{20}Ne_{meas}$, using the following set of equations:

$$^4He_{atm} = {}^{20}\mathrm{Ne}_{meas} \times \alpha, \mathrm{where}\alpha\mathrm{isthesolubilityof}{}^4He/{}^{20}\mathrm{Neattherechargetemperature}(12 \pm 1^{\circ}C),$$

$$^3He_{atm} = {}^4He_{atm} \times \mathrm{R}_a \times 0.985, \mathrm{withtheatmospheric}{}^3He/{}^4\mathrm{HeratioR}_a = 1.38 \times 10^{-6},$$

$$^3He_{ter} = ({}^4He_{meas} - {}^4He_{atm}) \times R_{ter} \mathit{where} R_{ter} \mathrm{standsfortheisotopicratioofradiogenicheliumproductioninrocks, setinthisworkatthetypicalvalueof} 2.0 \pm 0.5 \times 10^{-8}.$$

The overall uncertainty in the apparent $^3H/^3He$ ages is about 3 years in the case of this study.

3. Results

3.1. Hydrodynamic and chemical characterization of the study period

3.1.1. Hydrological conditions

Contrasted hydrological conditions were observed leading to differentiate two hydrological periods and one particular recharge event on the whole data set. The two first cycles (2005 and 2006) have precipitations below the mean inter-annual value (Fig. 2A) and correspond to a dry period. During this period, daily water table variations are low even during the recharge period. From 2007 to 2010, precipitations are higher or equal to the inter-annual value and characterize a humid period. Water table shows high daily variations in the early stage of the recharge periods (Fig. 2C). In particular, the hydrological year 2007 is characterized by intense precipitation inducing a very sharp increase of water table at the beginning of the recharge period (fall 2006). However, according to Ruiz et al. (2002b), on average, the fast flow associated with such storm events represents only 10% of the total annual flux.

Groundwater level shows high amplitude of seasonal variations. Upslope, close to the watershed divide, (nest H; Fig. 2B), water table depth varies from 5.5–6 m to 2–3 m during the hydrologic cycle. The permanently unsaturated zone is thus about 3 m thick. The aquifer remains permanently saturated up to 6 m below ground level. Water table level is slightly deeper downslope (nest J and L; Fig. 2B) but fluctuations observed upslope (nest H) and downslope (L) show a similar pattern. Midslope nest (J) shows a slightly different pattern with sharper fluctuations and the deepest water table level at the end of the recession period reflecting lower permeability in this area.

3.1.2. Influence of recharge and recession periods on groundwater chemistry

As previously reported Cl^- and NO_3^- show important annual variations (Fig. 2C, NO_3^- not shown) which contrast with the relative stability of the inter-annual values (Legout et al., 2007; Ruiz et al., 2002b). During the early stage of recharge periods shallow piezometers show a sharp decrease of Cl^- concentrations particularly visible for the recharge event of fall 2006. Such Cl^- drops indicate rapid circulations through the vadose zone inducing important dilution effect down to 6 m depth. Such events can be characterized as "by-pass" events. After 2007, the lack of data for these piezometers does not allow the observation of a similar evolution. However, a similar sharp decrease has been recorded on conductivity (not shown), confirming the dilution effect for early stages of recharge period. Then, after 2006, Cl^- variations follow water table fluctuations: during second stage of recharge period, Cl^- concentration increases when water level increases and reaches the highest Cl^- concentration at the end of the recharge periods (Fig. 2C). This variation has been previously suggested to be related to soil and regolith matrix contribution (Legout et al., 2007).

During recession period, Cl^- concentration decreases following water table decreases and reaches the lowest Cl^- concentration of the cycle. Cl^- variations are observed both in unsaturated and saturated zone down to 15 m but the variations are larger for shallow piezometers. In contrast, the deepest piezometer (F; 20 m depth), which presents the lowest Cl^- concentration, shows almost no annual variation. This evolution shows that the deep part of the saturated zone is not affected by preferential vertical flow path and thus, its chemical composition can be considered as representative of the groundwater end-member to interpret the highly variable chemical composition of shallow piezometers. As the dynamic of Cl^- concentration is particularly visible during the 2006–2007 cycle, we will therefore focus on this cycle.

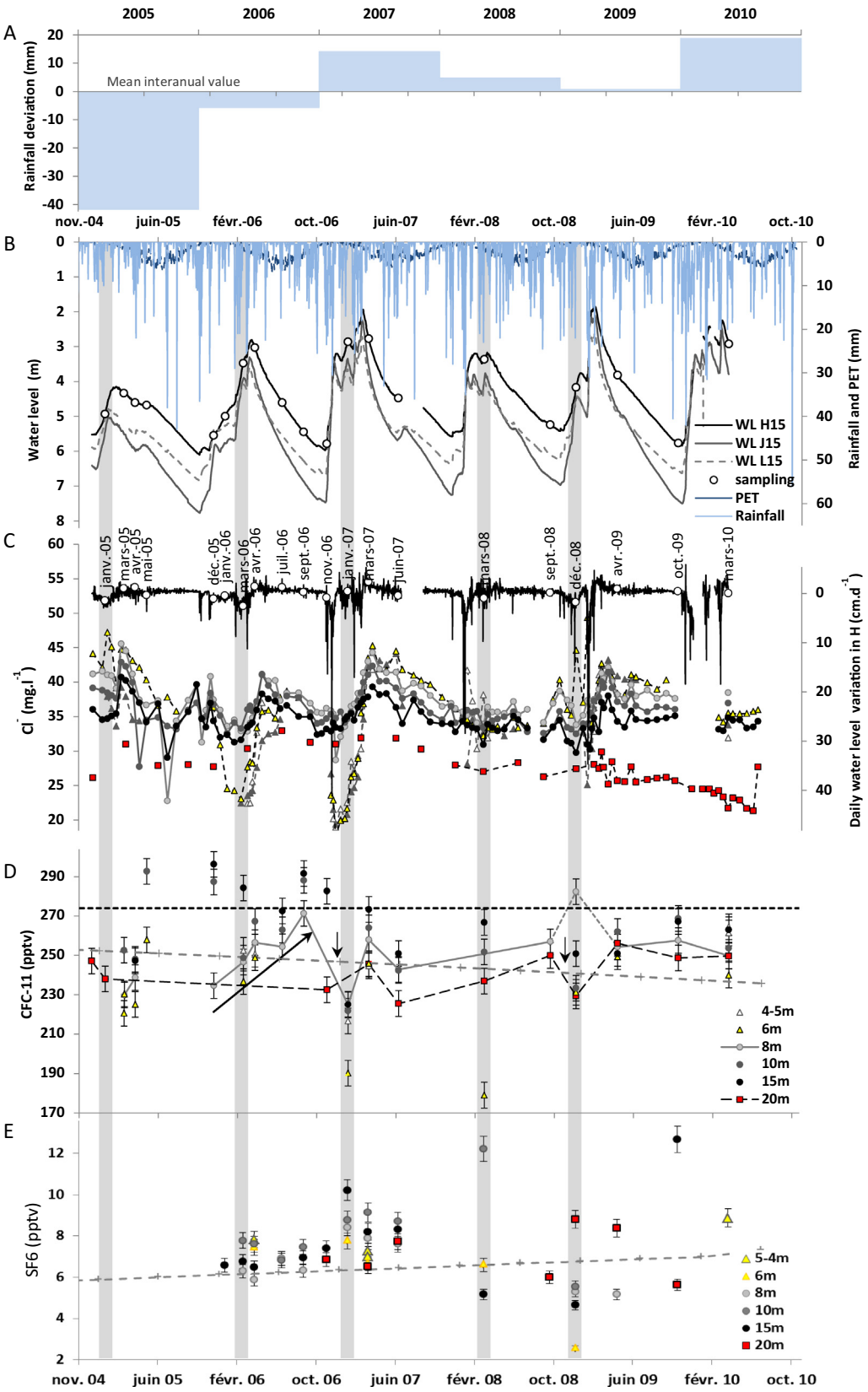

Fig. 2. Temporal evolution of precipitation, hydrogeology and hydrochemical parameters (Cl^-, CFC-11, SF6) of the system. (A) Annual precipitation deviation in comparison to the mean interannual precipitation over the year 2005 to 2010; (B) groundwater depth time series from the soil surface at nest H (upslope), J (midslope) and L (downslope), precipitation and potential evapotranspiration at the soil surface time series. Sampling periods have been reported on the water level and water level variation in H (white circle). (C) Cl-concentration ($mg{\cdot}L^{-1}$) and (D) CFC-11 and SF6 dissolved concentrations (pptv) respectively measured from January 2005 to October 2010 at different depth in nest H (upslope) and F compared to daily water level variation (in cm.d-1) in H15. (E) SF6 dissolved concentrations (pptv) respectively measured from January 2005 to October 2010 at different depth in nest H (upslope) and F. The dash lines (D-E) show the maximum mixing ratio in the atmosphere (black line) and the present mixing ratio (grey line). Main recharge period have been highlighted in grey.

3.2. Recharge temperature and excess air in groundwater

Fig. 3 shows the recharge temperature and excess air derived from the Ne, Ar and N_2 concentrations. Recharge temperatures range from 7.5 to 17 °C with most of the data between 7.5 and 12.5 °C i.e. with a wide range reflecting the soil temperature along the whole year. Excess air ranges from 0 to 0.02cm^{3}STP·g^{-1}. The results show small variations with depth. Shallow piezometers tend to have low excess air and slightly higher recharge temperature while at 15 and 20 m depth, excess air is slightly higher. However, a clear correlation with the hydrological regime could be observed. There is a global positive correlation between temperature and excess air, especially for samples from a recharge or discharge period. In general, samples with high NGT and low EA correspond at the end of recharge process (black squares; Fig. 3; Fig. 2: March07, March08, and April09).

3.3. Gas tracer distribution in groundwater

Table 1 summarizes the data obtained for CFC-11, CFC-12, SF_6 and $^3H/^3He$ per nest and per depth. All CFCs concentrations are relatively high in the aquifer, close to atmospheric maximum. CFC-11 concentrations range from 180pptv to 297pptv with an average concentration of 252pptv. These values indicate young groundwater (<25 yrs of apparent age) in good agreement with the small size of this unconfined aquifer. The relative standard deviation (stdv/mean) is about 10% but tends to be lower for deep piezometer at the head of the catchment (piezometer F) indicating a higher stability of concentrations with depth. CFC-12 concentrations range from 241 to 571pptv with an average concentration of 492pptv. The relative standard deviation is slightly higher namely for H8 and H15 (Table 1). After correction from excess air, SF_6 concentrations are almost always above saturation with an average value of 7.4pptv (compared to atmospheric value of 6.99pptv in 2010). These high values most probably reflect SF_6 lithogenic production within the weathered part of the aquifer. This interpretation is supported by batch leaching experiments of the Kerrien alterites that showed high SF_6 fluxes derived from the rock (Aquilina et al., 2010).

3.4. Spatial distribution

CFC-11 and CFC-12 mixing ratios show similar vertical profiles for the different nests (Fig. 4) suggesting that no clear evolution of the flow regime can be observed from upslope to downslope location of the catchment. CFC-11 vertical profile shows a decreasing concentration from 4 to 6 m depth with the lowest concentrations observed at 6 m depth. Then concentrations slightly increase up to 15 m. These variations are the highest for nest H. At the opposite, nest J shows the most constant vertical profile both in CFC-11 and CFC-12. As the scope of the paper is to give a better knowledge of recharge processes, we will then focus on detailed variations at nest H. To understand these profiles variation, it is necessary to have a closer look on the data evolution with time.

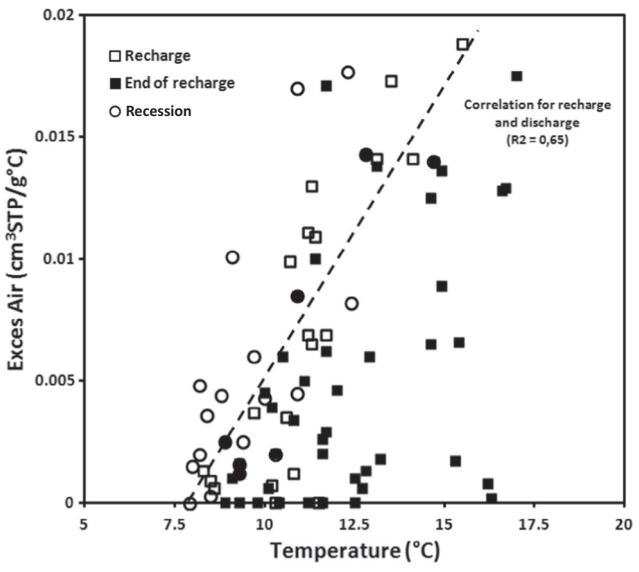

Fig. 3. Recharge temperature and excess air derived from gas concentrations.

3.5. Temporal variation

The long term monitoring (Fig. 2D) showed 2 clear trends in relation with the hydrologic condition. During the first dry cycles, in nest H, dissolved gases showed a general increase of their concentrations which is particularly pronounced from March06 to Sept06 (Fig. 2D). Moreover, several data present value above the atmospheric maximum. The occurrence of these high value disappeared after 2007. During the humid period, from 2007 to 2010 concentrations stabilize more or less between present atmospheric concentration and maximum concentrations with a slight increase trend for the deepest piezometer (20 m). Two important decreases of CFC-11 values were observed during recharge periods of January 2007 and December 2008. In detail, this observation leads to distinguish vertical patterns of recharge and recession periods (Fig. 5).

(1) During water table decrease (Apr and Jul06, March07, Apr09, Oct09 and March10), CFC-11 profiles were highly homogeneous with values ranging from 240 to 275pptv (Fig. 5B). Variation of CFC-11 concentration at the same depth was found to be very low. Two campaigns (May05 and Sept06) showed values above atmospheric maximum. The origin of these high values is not fully understood yet.

(2) During recharge event, CFC-11 profiles showed lower values and a higher variability especially in the water table fluctuation zone (4 to 8 m; Fig. 5A). For instance, the particular recharge event of January 2007 is marked by a sharp decrease of CFC-11 concentrations for all nests and depth down to 15 m, correlated to the fast water table increase and Cl^- decrease (Fig. 2C). The lowest gases values were observed at 6 m depth. The lack of gas data at 20 m depth does not allow concluding on the maximum depth of influence. This concentrations fall was also noticeable for CFC-12 in a lesser extent. A similar phenomenon was recorded during the recharge period of 2008 but to a lesser extent. This observation could explain the difference of global CFCs vertical profiles (Fig. 4).

3.6. Apparent age and flow model distribution

Mean apparent $^3H/^3He$ ages per depth range from 1.3 to 10.3 years with standard deviation ranging from 0.8 to 2.9 based on replicate samples (Table 1). Fig. 6A compares apparent $^3H/^3He$ ages and CFC-11 ages derived from piston flow model. Although CFCs and $^3H/^3He$ ages present discrepancies, ages given by the 2 methods are in the same order of magnitude (<25yrs) and both present a general increase with depth. In detail, results show that for shallow depth down to 10 m, most of CFC-11 provide similar or younger values than $^3H/^3He$, lower than 5yrs (Fig. 6). On the contrary, for the 15–20 m depth, CFC-11 apparent ages appear older than $^3H/^3He$ (about 20yrs for CFC-11 vs 5-12yrs for $^3H/^3He$) and a gap of CFC-11 ages can be observed between 12 and 18yrs. Part of this discrepancy can be due to the use of the piston flow model. At 15–20 m, as apparent $^3H/^3He$ is about 10 years old, CFC data fall at the maximum of the atmospheric mixing curves, increasing uncertainty in apparent age determination. The systematic use of the rising part of the atmospheric curve could have biased old the apparent CFC piston ages.

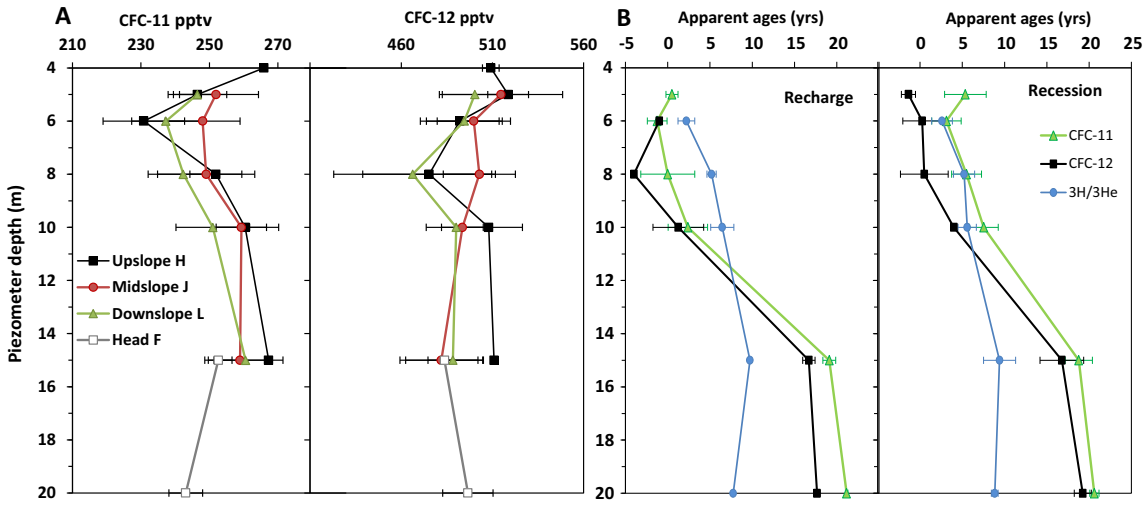

Fig. 4. Vertical profiles of CFC-11 and CFC-12 concentration at nests H (upslope), J (midslope) and L (downslope) (A) and corresponding apparent age evolution (B). Apparent $^{3}H/^{3}He$ age vertical profile has also been reported (B). Bars indicate the coefficient of variation between the different sampling.

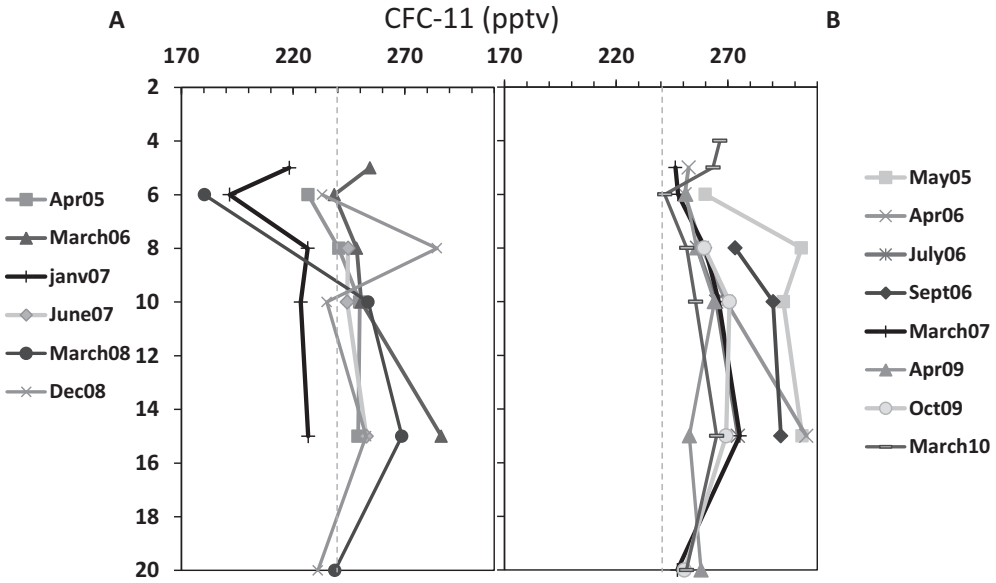

Fig. 5. Comparison of CFC-11 vertical profiles (y-axis unit is m) for (A) recharge period; and (B) recession period. Sampling periods with <3 depths have not been represented. Dashed line represent equilibrium concentration in 2010; maximum equilibrium concentration is 274pptv (1994).

Measured concentrations of CFC-11 and CFC-12 were compared with theoretical curves of different lumped parameter models (piston flow PFM, exponential mixing EMM, and binary mixing BMM; Fig. 7). Data fit in the higher part of the curves again indicating young groundwater of <25yrs. Numerous points appeared out of the curves indicating discrepancies between the 2 tracers. The CFC-11 values above the PFM curve correspond to the 2 first years of sampling that showed data above the atmospheric maximum indicating CFC-11 contamination. In contrast, low CFCs concentrations obtained during the special recharge event of January 2007 (and December 2008 at a lower degree) are shifted down and plotted out of the model curves (Fig. 7B). This is particularly visible for shallow depth (4,5–6 m, Fig. 7A). The other groundwater samples show mixed characteristics with data however mostly limited by a mixing line of present water and water recharge in 1988 (20yrs old). Taking into account the uncertainties, two main models explain most of the data: a piston model and an exponential mixing model.

We calculate CFC-11 MRT using an exponential model (EM). When no ages could be determined by EM (concentration higher than the maximum of the exponential curve), ages were derived from PFM. For young samples, similar ages were obtained with both models. For samples from 20 m only exponential ages could be obtained. Finally, recession periods were better explained by piston flow model.

The resulted MRT is presented versus $^{3}H/^{3}He$ apparent age in Fig. 6 B and C. A better agreement of CFC MRT and $^{3}H/^{3}He$ ages is obtained (Fig. 6B), with most of CFC MRT below 12yrs, in better accordance with $^{3}H/^{3}He$ apparent age. In particular, MRT from recession periods were in good agreement with $^{3}H/^{3}He$ apparent age (Apr09, Oct09; Fig. 6C). However, some CFC MRT, still appear older than $^{3}H/^{3}He$ apparent age, with no apparent correlation with depth. When looking at the hydrological period (Fig. 6C), it appears that CFC MRT that are older than $^{3}H/^{3}He$ age correspond to the Dec08 recharge event. Similarly, CFC MRTs from recharge events of Jan07 appear still older than average apparent $^{3}H/^{3}He$ ages

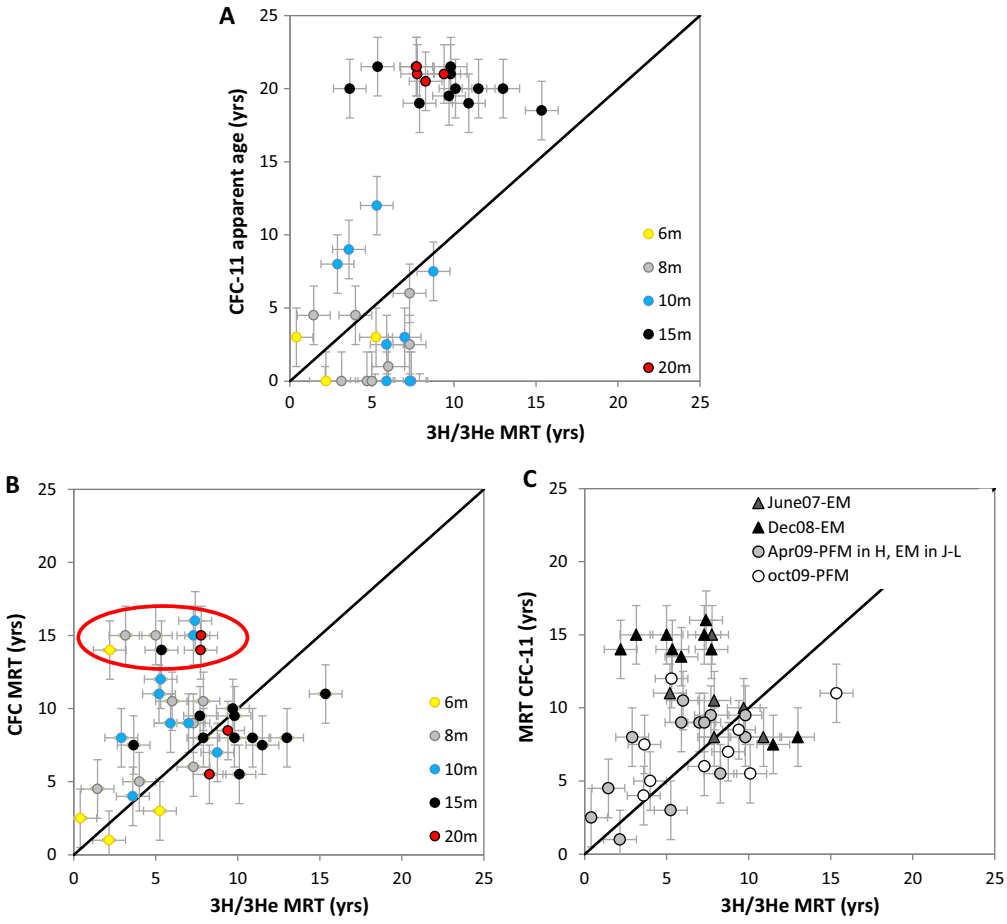

Fig. 6. Comparison of $^{3}H/^{3}He$ and CFC-11 apparent ages at different depths, assuming a piston fow model for CFCs ages (A). Considering the discrepancy at 15–20 m, CFC-11 ages have been determined using the best fitted model between EM or PFM and compared to $^{3}H/^{3}He$ apparent ages according to depth (B) and the period of sampling (C).

(about 15yrs even at shallow depth). For these events the type of lumped parameter model used to obtain MRT is not the origin of the discrepancy.

4. Discussion

4.1. Uncertainty in gas concentration estimation

The results show that ages obtained by $^{3}H/^{3}He$ and CFCs methods are in the same order of magnitude. Nevertheless, like in other studies combining these 2 age tracers, some discrepancies are observed (Happell et al., 2006; Kaown et al., 2009; Martin et al., 2016; Rademacher et al., 2001). Younger $^{3}H/^{3}He$ ages could be attributed to diffusive loss of ^{3}He to the atmosphere at times of low water table (Solomon et al. 1993, in Cook et al., 1995; Delbart et al., 2016; Martin et al., 2016; Rademacher et al., 2001). This would "reset" the $^{3}He/^{3}H$ clock inducing younger ages than CFCs ages (Cook et al., 1996). Noble gases are more prone to re-equilibration than CFCs because of their higher diffusivity (Han et al., 2006). This phenomenon could be enhanced by the thin vadose zone of the study site. In this study, CFCs retardation effect within the unsaturated zone would probably have low impact due to the low thickness of the permanently unsaturated zone (few meters thick) (Cook et al., 2006). In contrast, matrix diffusion processes between preferential flow path and matrix could cause discrepancy between the different tracers as they do not have the same aqueous diffusion coefficient (Cook et al., 2006). This phenomenon could explain why the apparent age derived from CFCs is higher than the water age derived from $^{3}H/^{3}He$.

Finally, the discrepancy could result from equilibration temperature that induced uncertainty in CFCs age calculation with older CFCs ages if recharge temperature is set too high. In this study we found differences in recharged temperature derived from NGT and Mean Annual Air Temperature. Such discrepancy has already been reported by Hall et al. (2005). They show that the lower NGTs compared to MAAT could reflect potential degassing or the time necessary for the waters to equilibrate. This is probably the case for groundwater showing little excess air. In both cases as observed by Hall et al. (2005), NGTs may be influenced by hydrological conditions. Such influence may explain the correlation between excess air and recharge temperature as well as the sampling-time, i.e. hydrological conditions dependency. This result requires further research but supports the interpretation of gas data as tracers of recharge processes.

4.2. Influence of position along the hillslope

Contrary to studies in a similar context (Gooddy et al., 2006; Newman et al., 2010), gas concentrations do not indicate clear variations of flow regime down gradient through the catchment (Fig. 4). This is consistent with the conclusion of a recent modelling study in a similar catchment (Molénat et al., 2013) where simulated CFCs groundwater mixing ratios were found not sensitive to the position along the hillslope in the range of the simulated MRT. In detail, the highest CFC vertical variations for nest H indicate a higher sensitivity to infiltration. Nest L appears to have similar behavior than nest H while nest J shows more homogeneous concentration with depth suggesting better permeability of the system. This slightly different

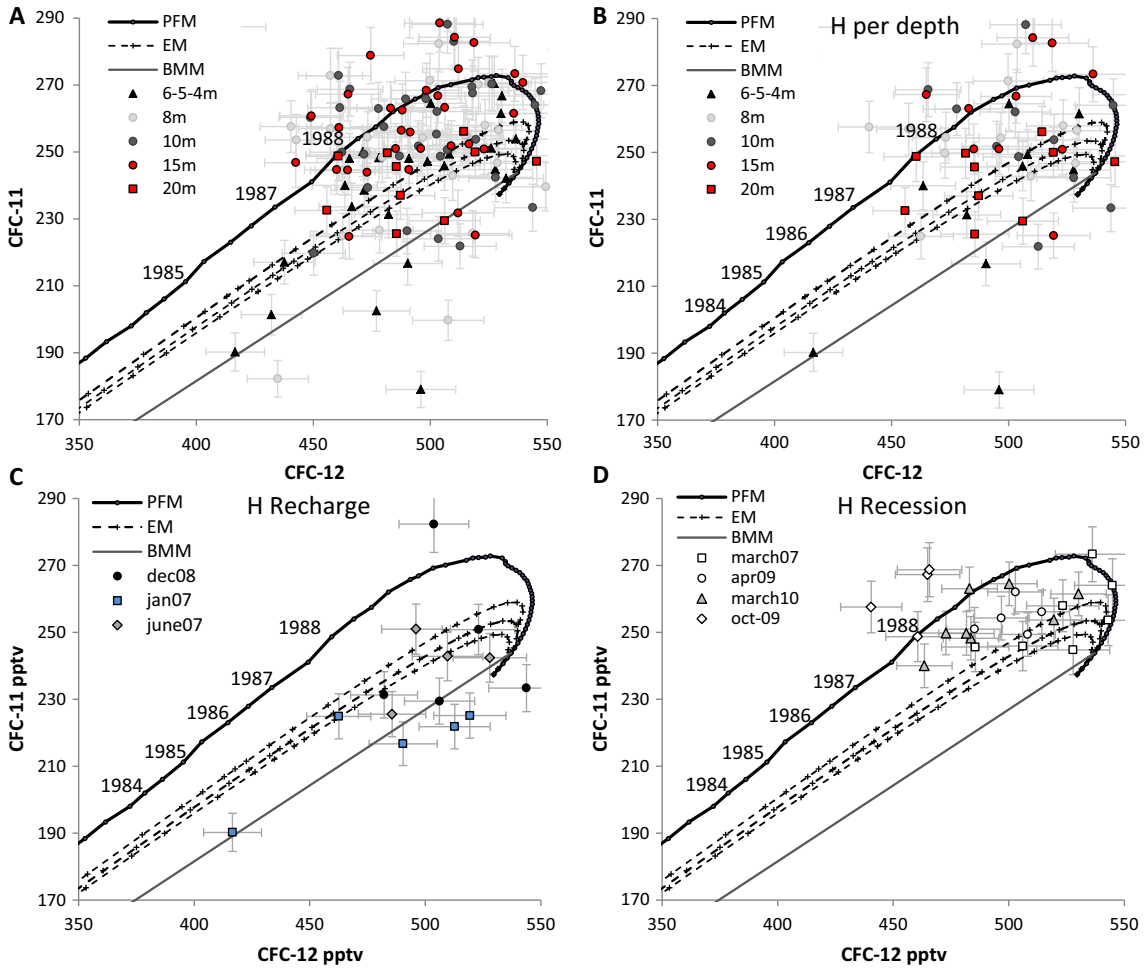

Fig. 7. CFC-11 and CFC-12 dissolved concentrations compared to flow models (Piston Flow Model (PFM); Exponential Model (EM) for sampling in 2005, 2007 and 2010; Binary Mixing Model (BMM)) depending on depth of sampling for all transect (A) or only plot H (B) or depending on the hydrological period in plot H: Recharge (C); Recession (D). During recharge, data are scattered below the model line.

physical property in nest J induces a lower influence of rapid infiltration which supports previous observations on spatial variation of water quality along the hillslope (Rouxel et al., 2011).

4.3. Influence of hydrologic condition on CFCs variability

At short time scale, the results show the influence of the sampling period on CFCs variability in groundwater. During low flow, there are small variations between different sampling periods (example of March07, March10 and Apr09) proving that one single time field sampling can be sufficient in most of cases. However, in this shallow aquifer, results show that recharge events have a strong impact on CFCs concentrations.

4.4. Processes influencing concentrations during beginning and end of recharge

The most representative example is the sampling during the recharge event of January 2007 and the following discharge period of March 2007. This sampling was done during a high recharge event after a dry period. At the beginning of the recharge period, diluted Cl^- concentrations reflect the infiltration of highly diluted rainwater through preferential flow path in the vadose zone. The dilution is observed on Cl^- down to 10 m. As a consequence, vertical Cl^- concentrations in groundwater reflect a mixing between permanent groundwater (35 mg/l) and rainwater (about 10 mg/l; Fig. 8B).

In Kerrien catchment, as the "old" permanent groundwater have similar CFC-11 mixing ratio than the atmosphere at the date of sampling (249pptv; Fig. 8A), mixing of permanent groundwater with rainwater should lead to a vertical homogeneous CFC-11 concentration close to the atmospheric concentration (Fig. 8A). Instead, CFC-11 concentrations show lower value with a sharp decrease between 6 and 8 m depth. The depleted values most probably reflect CFC-11 degradation as described in several studies for groundwater with anaerobic conditions (Cook et al., 2006, 1995; Darling et al., 2012; IAEA, 2006; Oster et al., 1996). This hypothesis is reinforced by the low DO values measured for sampling in January 2007 (4.5 mg/l). The maximum degradation is observed at 6–8 m depth which corresponds to the water table level during low flow. This observation is in good agreement with previous study that mentioned a denitrification zone down to 10 m in Kerrien catchment (Legout et al., 2005; Martin et al., 2006).

Before recharge, during low flow period, groundwater level is below 7 m depth. In the fluctuation zone, it is assumed that residual matrix water undergoes a chloride enrichment and CFC-11 degradation. During recharge, as water level rise in the fluctuation zone, permanent groundwater mixes with residual matrix water enriched in Cl^- and SF6 and depleted in CFC-11. In the same time, major infiltration of rainwater induces a decrease of Cl^- and limits the influence of CFC-11 degradation at shallow depth.

The major dilution effect on Cl^- down to 6 m reflects preferential flow paths and thus the heterogeneity of the aquifer. The

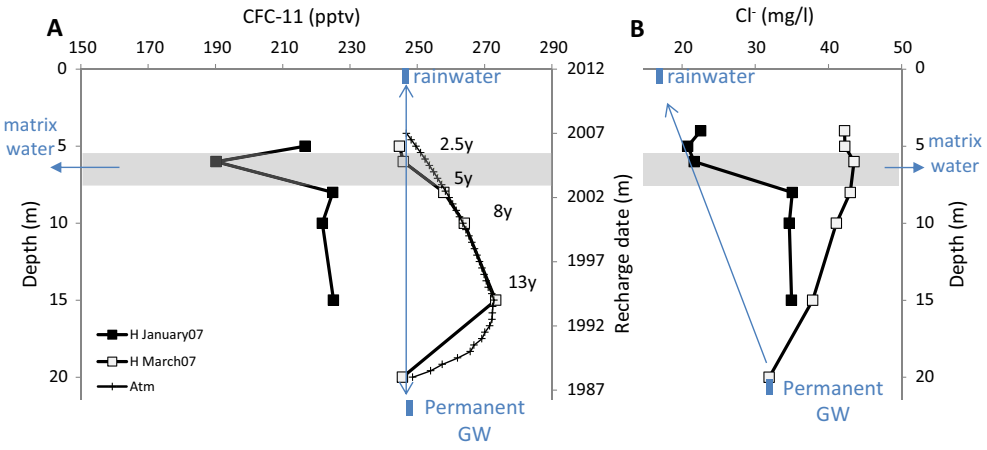

Fig. 8. CFC-11 (A) and Cl^- (B) profile in nest H during recharge event of January07 and following recession period (March07). Rainwater and permanent groundwater end-member are indicated by rectangles and their mixing by the arrow. Solid black line with crosses show the atmospheric mixing ratio of CFC-11 during the past 20 years.

contribution of the matrix water is supported by the increase of SF_6 values (up to 11.4pptv at 10 m vs 6.3pptv in the atmosphere in 2007). These SF_6 values in groundwater above atmospheric maximum reveal in situ production and confirm contribution of pore water with a higher contact time. Similar processes occur for the recharge event of December 2008 but to a less extent probably due to a lower water level rise during December 2008. Moreover the dry conditions during the 2 years before January 2007 are supposed to have enhanced the CFC-11 degradation process leading to undatable water samples.

At the end of recharge, (March07 or Apr09), vertical rainwater contribution has stopped as well as CFC-11 degradation since the system has been re-oxygenated. Shallow piezometers show high Cl^- concentrations. A decreasing influence of matrix contribution with depth explains the vertical Cl^- profile in nest H. During this recession period, except at 5–6 m depth, CFC ages can be estimated using a piston flow model (Fig. 6). CFC-11 profile shows a downward evolution with a modern value at the top of permanent saturated zone and an older value at the bottom in good agreement with the $^3H/^3He$ age profile. Similar results were obtained for April 2009. Such evolution indicates that mixing with matrix water occurs mainly at shallow depth down to 6–8 m, and then horizontal flows dominate in the system.

This interpretation is strengthened by the NGT and EA computation (Fig. 3). At the end of the recharge process, when Cl^- concentration is the highest, groundwater is characterized by relatively high NGT and lower EA. Such evolution in water chemistry can be explained by the contribution of pore water from the soil and the vadose zone. Although the potential mechanism remains unclear, such pore water closely bounded to the rock matrix would exclude air inclusion. During the beginning of the recharge process, most of the NGT show low value below 12 °C associated to relatively high EA which could reflect the rapid increase of water table due to the by-pass of "cold" rainwater.

4.5. Estimation of contribution from the different end-member

To validate the processes previously described, we did a first calculation using a 3 end-members mixing model: permanent groundwater, pore water and rainwater (Table 2). For rainwater, we used the atmospheric value of CFC-11 in 2007 and measured Cl^- value. For the permanent groundwater, we use CFC-11 value in F and Cl^- values in H15 during March 2007. The highest measured Cl^- concentration (49.4 mg/l in H6) was assumed to represent the Cl^- concentration in matrix water. Then we assumed a total degradation of CFC-11 leading to value close to 0pptv.

The observed Cl^- and CFC-11 values at 6 m were well simulated. During recharge period, a similar contribution of permanent groundwater and rainwater is found of about 40%. Matrix contribution is estimated to be up to 15%. At the end of recharge, rainwater contribution falls to 0. Shallow piezometers show high Cl^- concentrations that can be reproduced assuming a contribution of 50% of matrix water to permanent groundwater. Although, this computation can be only considered as a rough estimate, it confirms the influence of pore water contribution and indicates that vertical transfer are not negligible in the upper 6–8 of the groundwater section. A specific modelling should be carried out to further investigate the amplitude of this mechanism and potential effect in larger aquifers.

This interpretation shows that *i*) CFCs do not show a constant evolution during the hydrologic cycle and *ii*) different conceptual flow models have to be considered depending on depth and sampling period. During recharge, vertical flow and mixing dominate, limiting the use of apparent ages. In contrast, during recession periods, horizontal flows dominate and ages can be derived from piston classical flow models. At greater depth (20 m), tracer ages are obtained using exponential model showing that horizontal flows dominate and recharge event has low influence. This is consistent with previous results in similar context where the decrease in apparent ages below 10 m was attributed to groundwater moving horizontally through a second flow system (Cook et al., 1996). As a consequence, in such systems, the use of these classical models to estimate groundwater ages from atmospheric tracers should be limited to recession periods. This long-term monitoring shows that a good confidence can be given to apparent age at this period, with a difference of 2.8 yrs (±2.9) for the 8–10 m depth interval for 3 samplings with similar hydrological conditions (March07, Apr09 and March10). It is worth noting that the impact of the recharge period tends to disappear rapidly.

Table 2
End-members values and their respective contribution in H6 for a recharge period (January 2007) and an end of recharge period (March 2007).

	Permanent groundwater	Matrix Water	Rainwater	H6 recharge Jan07	H6 end of recharge March07
Cl^- (mg/l)	35	50	8	25.1	42.5
CFC-11 (pptv)	249	0	247	210.75	261.5
Contribution (Recharge)	40%	15%	45%		
Contribution (End of recharge)	50%	50%	0%		

4.6. Temporal distribution of mean residence time

In the previous sections, we mainly focused on one hydrological cycle to understand groundwater mechanisms. Here we examine the tracer ages obtained at each depth for all the investigated period (Fig. 9). Recharge samples (Jan07 and Dec08) presenting CFCs degradation were not used here. A general increase of MRT with depth is observed. It corresponds to an overall vertical groundwater velocity of 0.5 to 0.7 m per year, which is in good agreement with values obtained from previous tracing experiments in this system (Legout et al., 2007) and studies in similar geological context (Cook et al., 1996). However, a vertical layering of the groundwater MRTs is observed (Fig. 9). In the 0 to 6 m depth piezometers, i.e. within the water table fluctuation zone, very short to a few years MRT are observed. In the 8 to 10 m depth piezometers, the MRT range from a few years to a decade, while they increase to 10 to 15 years in the 15 to 20 m depth piezometers. This layering corresponds to the Cl^- vertical profile which shows a decreasing variability of concentration with depth (Rouxel et al., 2011).

The long term monitoring showed the effect of annual recharge on the residence time of the groundwater.

Present water only appears just after recharge periods very close to the water table. During the recession periods, even at the water table surface, the MRT is already close to 2.5 years (March05, Apr09) and water shows high Cl^- concentrations which confirms the influence of long-term residence time pore water from the unsaturated zone. At 8–10 m during the dry period (2005–2006 cycle), we show that groundwater is rejuvenated as water level increases. During recession, residence time tends to increase up to about 12 years as less rainwater enters in the system. The January 2007 special event highly modifies the system since a high amount of young water enters the system. In consequence, during the humid period, MRT are much younger with a mean value about 5yrs. At 15 m depth the MRTs are more stable than above. However the influence of the strong recharge event of January 2007 can still be observed: residence time is about 10-12yrs before January but decreases after January and stabilizes at 8yrs during 2008 and 2009 cycles.

At 20 m, during the dry period, a slight increase of residence time is observed in relation with a slight Cl^- increase. Then, residence times decrease from June 2007 to April 2009 and stabilize at 8yrs indicating that young water rejuvenates slowly the system at this depth. This rejuvenation explains the observed decrease of Cl^- concentration since January 2007 (Fig. 2). This observation confirm that groundwater at 20 m behaves relatively independently from other depths.

4.7. Consequences for conceptual model of the catchment

The highly similar pattern observed for both CFCs and Cl^- concentrations and the synchronous variations during recharge at depth of 5–15 m highlight the occurrence of vertical transfer from the variably saturated zone (2–6 m) down to 10–15 m depth. These results contradict the usual consideration of a major horizontal transfer from up to downslope as assumed by the approximation of Dupuit-Forsheimer which neglects vertical flows. These results also confirm that a double flow system can explain temporal variation in anionic concentrations as suggested previously (Legout et al., 2007; Rouxel et al., 2011). In addition, this work gives a better understanding of the mechanism controlling recharges. Local vertical downward flows occur during high recharge period inducing temporal variability in the anionic concentration of the permanent groundwater. High CFC-11 degradation at shallow depth (and CFC-12 to a lesser extent) indicates that during infiltration, rainwater

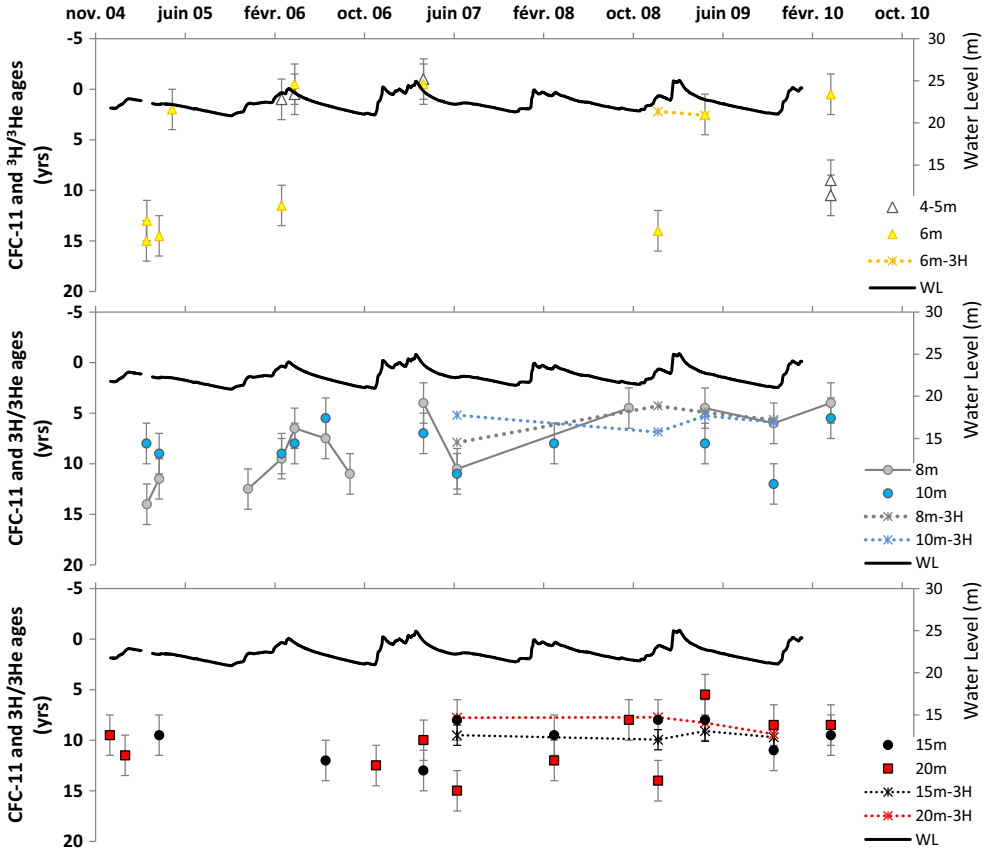

Fig. 9. Time series of ages derived from CFC-11 and $^3H/^3He$ for the unsaturated zone (4–6 m) and the permanent groundwater (8 m, 10 m, 15 m, 20 m).

mixes with evolved water from the matrix. As contribution of rainwater decreases, evolved matrix water contribution increases leading to Cl^- increase. This phenomenon is observed only when a sufficient groundwater level is reached and is enhanced by previous dry conditions.

5. Conclusions

Using a detailed analysis of long-term time-series of dissolved gas tracers in a shallow aquifer, we investigated how tracer concentrations and associated residence times evolve with depth and which flow processes (by-pass/ PFM/EM/Mixing) explain these evolutions. The long-term monitoring of dissolved gases shows a good repeatability in the permanent saturated zone and more variable apparent ages in the water fluctuation zone dominated by mixing. CFCs and $^3H/^3He$ indicate young groundwater. SF_6 show concentrations above the mean atmospheric mixing ratio indicating lithological production which limits its utilization in this aquifer for groundwater dating.

In this study, we show that hydrologic conditions have more influence on dissolved gas concentration than the location along the hillslope. Two different flow processes have to be considered between recharge and recession periods. During water table decreases, CFC-11 vertical profiles are highly homogeneous. During recharge periods, CFC profiles show variable but lower CFCs values reflecting contribution of modern rainwater and of the weathered matrix with variable proportion at the beginning of recharge and at the end of recharge period. This conceptual model is consistent with Cl^- concentration as well as excess air and recharge temperature evolution during the hydrologic cycle. The small variations observed between the sampling periods during recessions show that a single field sampling during groundwater recession period can be sufficient in most cases to estimate MRT. A general increase of mean residence time with depth is observed at longer time scales. In addition, this study shows a clear stratification between the first meters below the water table which exhibit highly variable gas concentrations, and the deep part of the aquifer which is much more homogeneous. Such stratification indicates that hydrological processes strongly differ in the variably saturated zone which acts as a buffer. These results confirm the interest of CFCs as age dating tracers for shallow groundwater, but also as natural tracers to conceptualizing flow processes. In this way, this work confirms the interest of atmospheric tracers to better constrain conceptual hydrological models regarding to their ability to represent different processes according to the hydrological period. Finally, this work demonstrates the interest of long-term monitoring of dissolved gases in complex hydrogeological environment for a better understanding of the recharge processes, with specific recharge events that impact groundwater over several cycles.

Acknowledgements

This work received a financial support by the French National Research Agency (ANR) through the Systerra programme (Acassya project ANR-08-STRA-01), the EU-RDF INTERREG IVA France (Channel) - England programme (Climawat project), and the INSU-CNRS EC2CO programme (Aquadiv project). The investigations also benefited from the support of INRA and CNRS (Environmental Research Observatory AgrHys).

References

Aeschbach-Hertig, W., 2004. Excess air in groundwater: problems and opportunities. Annual Meeting of GSA, Denver.

Aeschbach-Hertig, W., Peeters, F., Beyerle, U., Kipfer, R., 2000. Palaeotemperature reconstruction from noble gases in ground water taking into account equilibration with entrapped air. Nature 405, 1040–1044.

Aquilina, L., de Montety, V., Labasque, T., Molénat, J., Ruiz, L., Ayraud-Vergnaud, V., Fourré, E., 2010. CFC and SF6 concentrations in shallow groundwater: implications for groundwater age determination. WRI-13, Guanajuato, 16-20 Août 2010. Water-Rock Interaction XIII proceedings.

Aquilina, L., Vergnaud-Ayraud, V., Labasque, T., Bour, O., Molenat, J., Ruiz, L., de Montety, V., De Ridder, J., Roques, C., Longuevergne, L., 2012. Nitrate dynamics in agricultural catchments deduced from groundwater dating and long-term nitrate monitoring in surface- and groundwaters. Sci. Total Environ. 435–436, 167–178. https://doi.org/10.1016/j.scitotenv.2012.06.028.

Ayraud, V., Aquilina, L., Labasque, T., Pauwels, H., Molenat, J., Pierson-Wickmann, A.-C., Durand, V., Bour, O., Tarits, C., Le Corre, P., Fourre, E., Merot, P., Davy, P., 2008. Compartmentalization of physical and chemical properties in hard-rock aquifers deduced from chemical and groundwater age analyses. Appl. Geochem. 23, 2686–2707. https://doi.org/10.1016/j.apgeochem.2008.06.001.

Basu, N.B., Jindal, P., Schilling, K.E., Wolter, C.F., Takle, E.S., 2012. Evaluation of analytical and numerical approaches for the estimation of groundwater travel time distribution. J. Hydrol. 475, 65–73. https://doi.org/10.1016/j.jhydrol.2012.08.052.

Böhlke, J.-K., 2002. Groundwater recharge and agricultural contamination. Hydrogeol. J. 10, 153–179. https://doi.org/10.1007/s10040-001-0183-3.

Böhlke, J.K., Denver, J.M., 1995. Combined use of groundwater dating, chemical, and isotopic analyses to resolve the history and fate of nitrate contamination in two agricultural watersheds, atlantic coastal plain. Maryland. Water Resour. Res. 31, 2319–2339. https://doi.org/10.1029/95wr01584.

Chatton, E., Aquilina, L., Pételet-Giraud, E., Cary, L., Bertrand, G., Labasque, T., Hirata, R., Martins, V., Montenegro, S., Vergnaud, V., Aurouet, A., Kloppmann, W., Pauwels, 2016. Glacial recharge, salinisation and anthropogenic contamination in the coastal aquifers of Recife (Brazil). Sci. Total Environ. 569–570, 1114–1125. https://doi.org/10.1016/j.scitotenv.2016.06.180.

Cook, P.G., Plummer, L., Solomon, D., Busenberg, E., Han, L., 2006. Effects and processes that can modify apparent CFC age. In: Use of Chloroflurocarbons in Hydrology: A Guidebook. IAEA, Vienna, pp. 31–58.

Cook, P.G., Solomon, D.K., Plummer, L.N., Busenberg, E., Schiff, S.L., 1995. Chlorofluorocarbons as tracers of groundwater transport processes in a shallow Silty Sand Aquifer. Water Resour. Res. 31, 425–434. https://doi.org/10.1029/94WR02528.

Cook, P.G., Solomon, D.K., Sanford, W.E., Busenberg, E., Plummer, L.N., Poreda, R.J., 1996. Inferring shallow groundwater flow in saprolite and fractured rock using environmental tracers. Water Resour. Res. 32, 1501–1509. https://doi.org/10.1029/96wr00354.

Creed, I.F., Band, L.E., 1998. Export of nitrogen from catchments within a temperate forest: evidence for a unifying mechanism regulated by variable source area dynamics. Water Resour. Res. 34, 3105–3120. https://doi.org/10.1029/98wr01924.

Darling, W.G., Gooddy, D.C., MacDonald, A.M., Morris, B.L., 2012. The practicalities of using CFCs and SF6 for groundwater dating and tracing. Appl. Geochem. 27, 1688–1697. https://doi.org/10.1016/j.apgeochem.2012.02.005.

Delbart, C., Barbecot, F., Valdes, D., Tognelli, A., Fourre, E., Purtschert, R., Couchoux, L., Jean-Baptiste, P., 2016. Investigation of young water inflow in karst aquifers using SF6-CFC-3H/He-85Kr-39Ar and stable isotope components. Appl. Geochem. 50, 164–176. https://doi.org/10.1016/j.apgeochem.2014.01.011.

Fovet, O., Ruiz, L., Faucheux, M., Molénat, J., Sekhar, M., Vertes, F., Aquilina, L., Gascuel-Odoux, C., Durand, P., 2015. Using long time series of agricultural-derived nitrates for estimating catchment transit times. J. Hydrol. 522, 603–617. https://doi.org/10.1016/j.jhydrol.2015.01.030.

Gooddy, D.C., Darling, W.G., Abesser, C., Lapworth, D.J., 2006. Using chlorofluorocarbons (CFCs) and sulphur hexafluoride (SF6) to characterise groundwater movement and residence time in a lowland Chalk catchment. J. Hydrol. 330, 44–52. https://doi.org/10.1016/j.jhydrol.2006.04.011.

Hall, C.M., Castro, M.C., Lohmann, K.C., Ma, L., 2005. Noble gases and stable isotopes in a shallow aquifer in southern Michigan: implications for noble gas paleotemperature reconstructions for cool climates. Geophys. Res. Lett. 32, L18404. https://doi.org/10.1029/2005GL023582.

Han, L.E., Groning, M., Plummer, L.N., Solomon, D.K., 2006. Comparison of the CFC technique with other techniques (3H, 3H/3He, 85Kr). Use of Chlorofluorocarbons in Hydrology: A Guidebook. IAEA, pp. 191–198.

Happell, J.D., Opsahl, S., Top, Z., Chanton, J.P., 2006. Apparent CFC and 3H/3He age differences in water from Floridan Aquifer springs. J. Hydrol. 319, 410–426.

Heaton, T.H.E., Vogel, J.C., 1981. "Excess air" in groundwater. J. Hydrol. 50, 201–216. https://doi.org/10.1016/0022-1694(81)90070-6.

Herzberg, O., Mazor, E., 1979. Hydrological applications of noble gases and temperature measurements in underground water systems: examples from Israel. J. Hydrol. 41, 217–231. https://doi.org/10.1016/0022-1694(79)90063-5.

Hrachowitz, M., Savenije, H.H.G., Blöschl, G., McDonnell, J.J., Sivapalan, M., Pomeroy, J.W., Arheimer, B., Blume, T., Clark, M.P., Ehret, U., Fenicia, F., Freer, J.E., Gelfan, A., Gupta, H.V., Hughes, D.A., Hut, R.W., Montanari, A., Pande, S., Tetzlaff, D., Troch, P.A., Uhlenbrook, S., Wagener, T., Winsemius, H.C., Woods, R.A., Zehe, E., Cudennec, C., 2013. A decade of Predictions in Ungauged Basins (PUB) – a review. Hydrol. Sci. J. 58, 1–58. https://doi.org/10.1080/02626667.2013.803183.

IAEA, 2006. Use of Chlorofluorocarbons in hydrology: A Guidebook, STI/PUB/1238. <http://www-pub.iaea.org/MTCD/publications/PDF/Pub1238_web.pdf>.

Jean-Baptiste, P., Fourré, E., Dapoigny, A., Baumier, D., Baglan, N., Alanic, G., 2010. 3He mass spectrometry for very low-level measurement of organic tritium in environmental samples. J. Environ. Rad. 101, 185–190.

Jean-Baptiste, P., Mantisi, F., Dapoigny, A., Stievenard, M., 1992. Design and performance of a mass spectrometric facility for measuring helium isotopes

in natural waters and for low-level tritium determination by the 3He ingrowth method. Appl. Radiat. Isot. 43, 881–891.
Kaown, D., Koh, D.-C., Lee, K.-K., 2009. Effects of groundwater residence time and recharge rate on nitrate contamination deduced from δ18O, δD, 3H/3He and CFCs in a small agricultural area in Chuncheon Korea. J. Hydrol. 366, 101–111. https://doi.org/10.1016/j.jhydrol.2008.12.016.
Katz, B.G., Böhlke, J.K., Hornsby, H.D., 2001. Timescales for nitrate contamination of spring waters, northern Florida, USA. Chem. Geol. 179, 167–186. https://doi.org/10.1016/s0009-2541(01)00321-7.
Kendall, C., McDonnell, J.J., 1998. Isotope Tracers in Catchment Hydrology. Elsevier Science Publishers, Amsterdam.
Kipfer, R., Aeschbach-Hertig, W., Peeters, F., Stute, M., 2002. Noble gases in lakes and ground waters. Rev. Mineral. Geochem. 47 (1), 615–700.
Kirchner, J.W., Feng, X., Neal, C., 2001. Catchment-scale advection and dispersion as a mechanism for fractal scaling in stream tracer concentrations. J. Hydrol. 254, 82–101. https://doi.org/10.1016/S0022-1694(01)00487-5.
Koh, D.-C., Niel Plummer, L., Kip Solomon, D., Busenberg, E., Kim, Y.-J., Chang, H.-W., 2006. Application of environmental tracers to mixing, evolution, and nitrate contamination of ground water in Jeju Island Korea. J. Hydrol. 327, 258–275. https://doi.org/10.1016/j.jhydrol.2005.11.021.
Kolbe, T., Marçais, J., Thomas, Z., Abbott, B.W., de Dreuzy, J.-R., Rousseau-Gueutin, P., Aquilina, L., Labasque, T., Pinay, G., 2016. Coupling 3D groundwater modeling with CFC-based age dating to classify local groundwater circulation in an unconfined crystalline aquifer. J. Hydrol. 543 (Part A), 31–46. https://doi.org/10.1016/j.jhydrol.2016.05.020.
Labasque, T., Vergnaud, V. and Aquilina, L., 2008. Recent methodology developed in Rennes (France) at Geosciences laboratory in groundwater dating using CFCs, SF6 and dissolved gases (Ne, Ar, O2, N2, CH4, CO2 and N2O). G-DAT 2008 proceedings, Leipzig, Germany.
Le Gal La Salle, C., Aquilina, L., Fourre, E., Jean-Baptiste, P., Michelot, J.L., Roux, C., Bugai, D., Labasque, T., Simonucci, C., Van Meir, N., Noret, A., Bassot, S., Dapoigny, A., Baumier, D., Verdoux, P., Stammose, D., Lancelot, J., 2012. Groundwater residence time downgradient of Trench No. 22 at the Chernobyl Pilot Site: Constraints on hydrogeological aquifer functioning. Appl. Geochem. 27, 1304–1319. https://doi.org/10.1016/j.apgeochem.2011.12.006.
Legout, C., Molenat, J., Aquilina, L., Gascuel-Odoux, C., Faucheux, M., Fauvel, Y., Bariac, T., 2007. Solute transfer in the unsaturated zone-groundwater continuum of a headwater catchment. J. Hydrol. 332, 427–441.
Legout, C., Molenat, J., Lefebvre, S., Marmonier, P., Aquilina, L., 2005. Investigation of biogeochemical activities in the soil and unsaturated zone of weathered granite. Biogeochemistry 75, 329–350.
Maloszewski, P., Zuber, A., 1982. Determining the turnover time of groundwater systems with the aid of environmental tracers. J. Hydrol. 57, 207–231. https://doi.org/10.1016/0022-1694(82)90147-0.
Martin, C., Aquilina, L., Gascuel-Odoux, C., Molénat, J., Faucheux, M., Ruiz, L., 2004. Seasonal and interannual variations of nitrate and chloride in stream waters related to spatial and temporal patterns of groundwater concentrations in agricultural catchments. Hydrol. Process. 18, 1237–1254. https://doi.org/10.1002/hyp.1395.
Martin, C., Molenat, J., Gascuel-Odoux, C., Vouillamoz, J.M., Robain, H., Ruiz, L., Faucheux, M., Aquilina, L., 2006. Modelling the effect of physical and chemical characteristics of shallow aquifers on water and nitrate transport in small agricultural catchments. J. Hydrol. 326, 25–42. https://doi.org/10.1016/j.jhydrol.2005.10.040.
Martin, J.B., Kurz, M.J., Khadka, M.B., 2016. Climate control of decadal-scale increases in apparent ages of eogenetic karst spring water. J. Hydrol. 540, 988–1001. https://doi.org/10.1016/j.jhydrol.2016.07.010.
Molénat, J., Davy, P., Gascuel-Odoux, C., Durand, P., 2000. Spectral and cross-spectral analysis of three hydrological systems. Phys. Chem. Earth Part B Hydrol. Oceans Atmosphere 25, 391–397. https://doi.org/10.1016/S1464-1909(00)00032-0.
Molenat, J., Durand, P., Gascuel-Odoux, C., Davy, P., Gruau, G., 2002. Mechanisms of nitrate transfer from soil to stream in an agricultural watershed of French brittany. Water. Air. Soil Pollut. 133, 161–183. https://doi.org/10.1023/a:1012903626192.
Molénat, J., Gascuel-Odoux, C., 2002. Modelling flow and nitrate transport in groundwater for the prediction of water travel times and of consequences of land use evolution on water quality. Hydrol. Process. 16, 479–492. https://doi.org/10.1002/hyp.328.
Molénat, J., Gascuel-Odoux, C., Aquilina, L., Ruiz, L., 2013. Use of gaseous tracers (CFCs and SF6) and transit-time distribution spectrum to validate a shallow groundwater transport model. J. Hydrol. 480, 1–9. https://doi.org/10.1016/j.jhydrol.2012.11.043.
Molenat, J., Gascuel-Odoux, C., Ruiz, L., Gruau, G., 2008. Role of water table dynamics on stream nitrate export and concentration in agricultural headwater catchment (France). J. Hydrol. 348, 363–378. https://doi.org/10.1016/j.jhydrol.2007.10.005.
Neal, C., Kirchner, J.W., 2000. Sodium and chloride levels in rainfall, mist, streamwater and groundwater at the Plynlimon catchments, mid-Wales: inferences on hydrological and chemical controls. Hydrol. Earth Syst. Sci., 295
Newman, B.D., Osenbrück, K., Aeschbach-Hertig, W., Kip Solomon, D., Cook, P., Różański, K., Kipfer, R., 2010. Dating of 'young' groundwaters using environmental tracers: advantages, applications, and research needs. Isotopes Environ. Health Stud. 46, 259–278. https://doi.org/10.1080/10256016.2010.514339.
Oster, H., Sonntag, C., Münnich, K.O., 1996. Groundwater age dating with chlorofluorocarbons. Water Resour. Res. 32, 2989–3001. https://doi.org/10.1029/96wr01775.
Rademacher, L.K., Clark, J.F., Hudson, G.B., Erman, D.C., Erman, N.A., 2001. Chemical evolution of shallow groundwater as recorded by springs, Sagehen basin; Nevada County, California. Chem. Geol. 179, 37–51. https://doi.org/10.1016/S0009-2541(01)00314-X.
Rouxel, M., Molénat, J., Ruiz, L., Legout, C., Faucheux, M., Gascuel-Odoux, C., 2011. Seasonal and spatial variation in groundwater quality along the hillslope of an agricultural research catchment (Western France). Hydrol. Process. 25, 831–841. https://doi.org/10.1002/hyp.7862.
Rouxel, M., Ruiz, L., Molenat, J., Hamon, Y., Chirie, G., Michot, D., 2012. Experimental determination of hydrodynamic properties of weathered granite. Vadose Zone J. 11, 10. https://doi.org/10.2136/vzj2011.0076.
Ruiz, L., Abiven, S., Durand, P., Martin, C., Vertes, F., Beaujouan, V., 2002a. Effect on nitrate concentration in stream water of agricultural practices in small catchments in Brittany: I. Annual nitrogen budgets. Hydrol. Earth Syst. Sci. 497.
Ruiz, L., Abiven, S., Martin, C., Durand, P., Beaujouan, V., Molénat, J., 2002b. Effect on nitrate concentration in stream water of agricultural practices in six small catchments in Brittany: II. Temporal variations and mixing processes. Hydrol. Earth Syst. Sci. 6, 507–513.
Schlosser, P., Stute, M., Sonntag, C., Münnich, K.O., 1989. Tritiogenic 3He in shallow groundwater. Earth Planet. Sci. Lett. 94 (3–4), 245–256.
Stute, M., Forster, M., Frischkorn, H., Serejo, A., Clark, J.F., Schlosser, P., Broecker, W. S., Bonani, G., 1995. Cooling of tropical Brazil (5 °C) during the last glacial maximum. Science 269, 379–383. https://doi.org/10.1126/science.269.5222.379.
Suckow, A., 2014. The age of groundwater: definitions, models and why we do not need this term. Appl. Geochem. 50, 222–230. https://doi.org/10.1016/j.apgeochem.2014.04.016.